Supporting information for

Anti-poisoned oxygen reduction reaction by rice-like Pd-Sb nanoparticles

Hui Fu,[a] Yao Chen,[a] Shuanglong Lu,[a] Zhe Zhang,[a] Ting Zhu,[b] Hanjun Li,[a] Feili Lai,*[c] Nan Zhang*[a] and Tianxi Liu*[a]

[a] Key Laboratory of Synthetic and Biological Colloids, Ministry of Education, School of Chemical and Material Engineering, International Joint Research Laboratory for Nano Energy Composites, Jiangnan University, Wuxi, 214122, China.

[b] *National Laboratory of Solid-State Microstructures/School of Electronics Science and Engineering/Collaborative Innovation Center of Advanced Microstructures, Nanjing University, Nanjing, 210093, China.*

[c] *Department of Chemistry, KU Leuven, Celestijnenlaan 200F, Leuven 3001, Belgium.*

E-mail: feili.lai@kuleuven.be, nzhang@jiangnan.edu.cn, txliu@jiangnan.edu.cn

Experimental section:

Chemicals. Palladium (II) acetylacetonate ($Pd(acac)_2$), polyvinylpyrrolidone (PVP, MW = 58000), oleylamine (OAm, 68-70%), palladium (II) chloride ($PdCl_2$), and antimony (III) triacetate ($Sb(ac)_3$) were purchased from J&K China Chemical Ltd (Shanghai, China). Antimony (III) trichloride ($SbCl_3$) was purchased from Shanghai Aladdin Biochemical Technology Co., Ltd. Ammonium bromide (NH_4Br), ammonium chloride (NH_4Cl), ammonium iodide (NH_4I), N,N-dimethylformamide (DMF), N,N-dimethylacetamide (DMAC), and ethylene glycol (EG) were purchased from Sinopharm Chemical Reagent Co. Ltd (Shanghai, China). Oleic acid (OA, ≥99%) and tri-n-octylphosphine ($C_{24}H_{51}P$) were purchased from TCI (Tokyo, Japan). The deionized water (H_2O) (18 MΩ cm^{-1}) used in all experiments was prepared by (or passing water through) an ultra-pure purification system (Aqua Solutions).

Synthesis of $Pd_{20}Sb_7$ nanoparticles (NPs). In a typical synthesis of $Pd_{20}Sb_7$ NPs, 7.4 mg of $Pd(acac)_2$, 3.9 mg of $SbCl_3$, 15 mg of NH_4Br, 200 mg of PVP, and 10 mL of DMF were added into a 30 mL of glass bottle. The mixture was ultrasonicated for around 0.5 h. The resulting homogeneous mixture was heated from room temperature to 180 °C and kept at 180 °C for 5 h in an oil bath. The resulting colloidal product was collected by centrifugation and washed with an ethanol/acetone mixture.

Synthesis of Pd NPs. In a typical synthesis of Pd NPs, 7.4 mg of $Pd(acac)_2$, 100 μL of $C_{24}H_{51}P$, 4 mL of OAm and 1 mL of OA were added into a vial (volume: 30 mL). After the vial had been capped, the mixture was ultrasonicated for around 0.5 h. The resulting homogeneous mixture was heated from room temperature to 160 °C and kept at 160 °C for 5 h in an oil bath. After cooling to room temperature, the colloidal products were collected by centrifugation and washed with a cyclohexane/ethanol mixture.

Characterization. Transmission electron microscopy (TEM) images were obtained using HITACHI HT7700 operating at 120 kV. High-resolution TEM (HRTEM) and high-angle annular dark-field scanning transmission electron microscope (HAADF-STEM) images were acquired on a FEI Tecnai F20 transmission electron microscope with an acceleration voltage of 200 kV. Powder X-ray diffraction (PXRD) patterns were collected by a X'Pert-Pro MPD diffractometer (Netherlands PANalytical) with a Cu Kα X-ray source (λ = 1.540598 Å). X-ray photoelectron spectroscopy (XPS) analysis was done with Axis supra (Kratos Analytical Ltd). The carbon peak at 284.8 eV was used as a reference to correct the charging effects. The concentration of catalysts was further determined by the inductively coupled plasma atomic emission spectroscopy (710-ES, Varian, ICP-AES). X-ray absorption fine structure (XAFS) measurements were carried out at the BL14W1 station in Shanghai Synchroton Radiation Facility (SSRF, 3.5 GeV, 250 mA in maximum, Si (311) double-crystals).

Electrochemical oxygen reduction reaction (ORR) measurements. A three-electrode cell was used for the electrochemical measurements. The rotating disk electrode (RDE) from Pine Instruments was used as the working electrode, a saturated calomel electrode (SCE) was used as the reference electrode and a carbon rod was used as the counter electrode, respectively. To prepare the catalyst-coated working electrode, the catalyst was dispersed in a mixture containing isopropanol and Nafion (5 wt%) to form a 0.20 mg_{Pd} mL^{-1} dispersion. 10 μL dispersion of $Pd_{20}Sb_7$ NPs/C (0.20 mg_{Pd} mL^{-1}) was deposited on a RDE to obtain the working electrode after the solvent was dried at room temperature. The cyclic voltammetry (CV) was carried out at room temperature in 0.1 M KOH solution. The potential scan rate was 50 mV s^{-1} for CV measurement. The ORR measurements were conducted in a 0.1 M KOH solution purged with O_2 during the measurement. The scan and rotation rates for ORR measurement were 10 mV s^{-1} and 1600 rpm,

respectively. The CH_3OH and CO tolerance tests were conducted at the same condition with ORR measurements but adding CH_3OH or CO into electrolyte, respectively. The anti-poisoning durability tests were performed at room temperature in O_2-saturated 0.1 M KOH by introducing 0.5 M CH_3OH or CO into the electrolyte at 200 s. All electrochemical experiments were performed at room temperature. For comparison, the as prepared Pd NPs/C and the commercial Pd/C were used as the baseline catalysts, and same procedures described above were applied to conduct the electrochemical measurements.

Gas diffusion electrode (GDE) measurements. The catalysts were dispersed in a mixture containing isopropanol and deionized water (v: v=1: 3) and Nafion (5 wt%) to form a 0.50 mg_{Pd} mL^{-1} dispersion. 10 μL of catalyst dispersion was deposited on the gas diffusion layer to form catalyst layer. The catalyst layer (0.2 cm^2), carbon rod, and SCE were used as the working electrode, counter electrode, and reference electrode, respectively. Before the ORR measurements, 50 CV cycles were applied at a scanning rate of 500 mV s^{-1} in 1 M KOH to activate the catalysts. Then, the ORR polarization curves were measured in the potential range from 0.06 V_{RHE} to 1.1 V_{RHE} with the sweep rate of 50 mV s^{-1} under conditions of slow O_2 flow rate. Using this setup, the humid gas was introduced into the GDE cell at room temperature.

Density functional theory (DFT) calculations. Geometric optimizations using periodic DFT were performed in the Vienna *ab initio* simulation package (VASP) within the plane wave method and generalized gradient approximation Perdew-Burke-Ernzerhof (GGA-PBE) functional.[1-3] Calculations were converged until energy and force components were less than 3×10^{-5} eV and 0.05 eV/Å, respectively. A 500-eV plane wave cutoff was applied for all calculations. The centered K points sampling in reciprocal space with $5 \times 1 \times 1$ mesh were used. The vacuum space was set as 10 Å in z coordinate to avoid the image interaction between periodic slabs. The Pd-terminal facet with the minimal dangling bond was chosen to be the surface model, as it closely relates to experiment. All the slabs were constructed with three layers of Pd-Sb-Pd composites, of which only the top one layer was allowed to relax.

References:

1. G. Kresse and J. Furthmüller, *Comput. Mater. Sci.* 1996, **6**, 15-50.

2. P. E. Blöchl, *Phys. Rev. B* 1994, **50**, 17953-17979.

3. J. P. Perdew, K. Burke and M. Ernzerhof, *Phys. Rev. Lett.* 1996, **77**, 3865-3868.

Supporting Figures and Table.

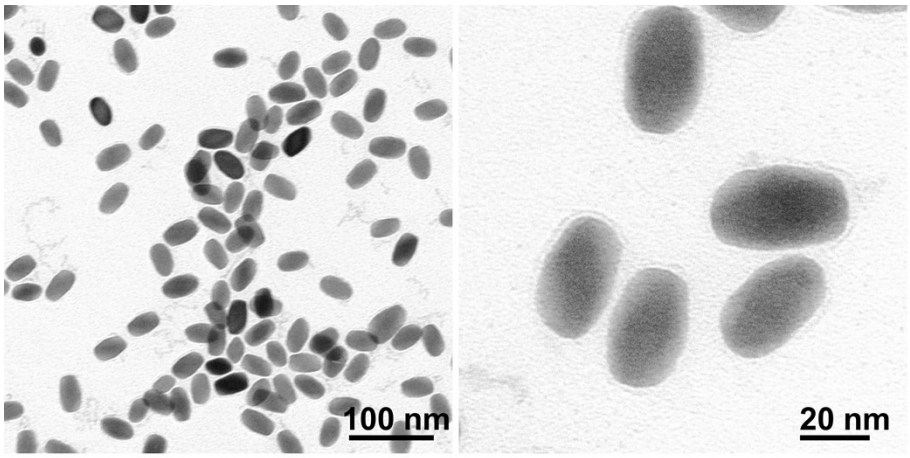

Fig. S1. TEM images of $Pd_{20}Sb_7$ NPs.

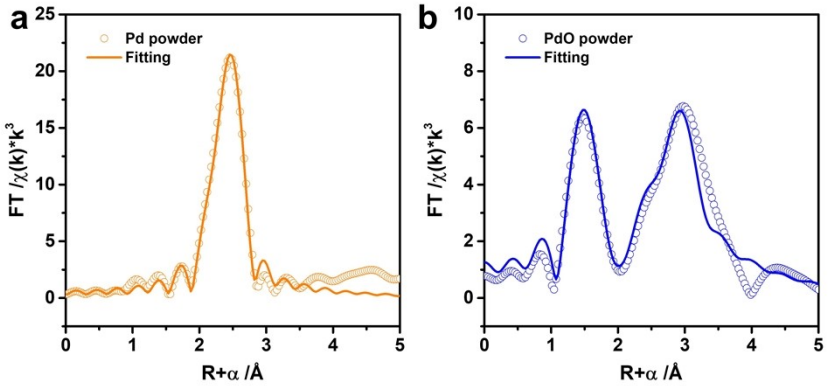

Fig. S2. Experimental and fitting data of Pd K-edge FT-EXAFS spectrum in R space for (a) Pd powder and (b) PdO powder.

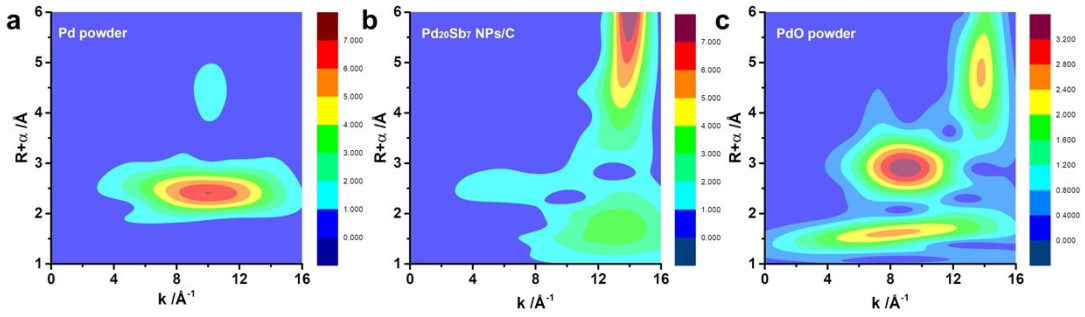

Fig. S3. WT analyses of the Pd K-edge FT-EXAFS data for (a) Pd powder, (b) $Pd_{20}Sb_7$ NPs/C, and (c) PdO powder.

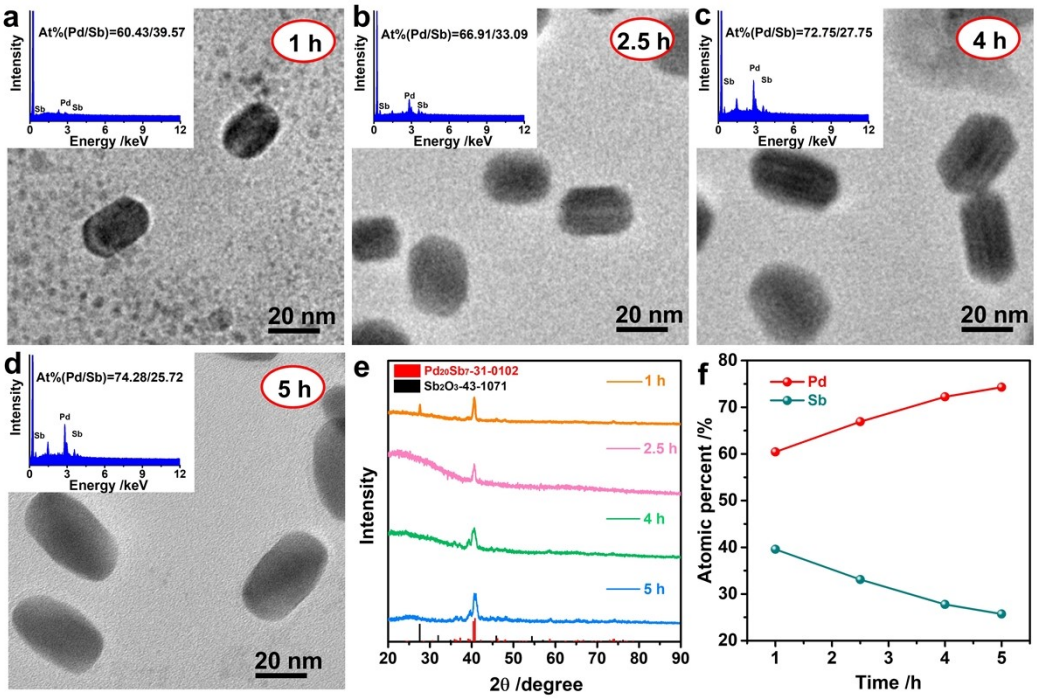

Fig. S4. TEM images of Pd-Sb NPs at different reaction times: (a) 1 h, (b) 2.5 h, (c) 4 h, (d) 5 h. (The insert images are SEM-EDS spectra at the corresponding times) (e) PXRD patterns and (f) SEM-EDS results of the intermediates produced at different reaction times.

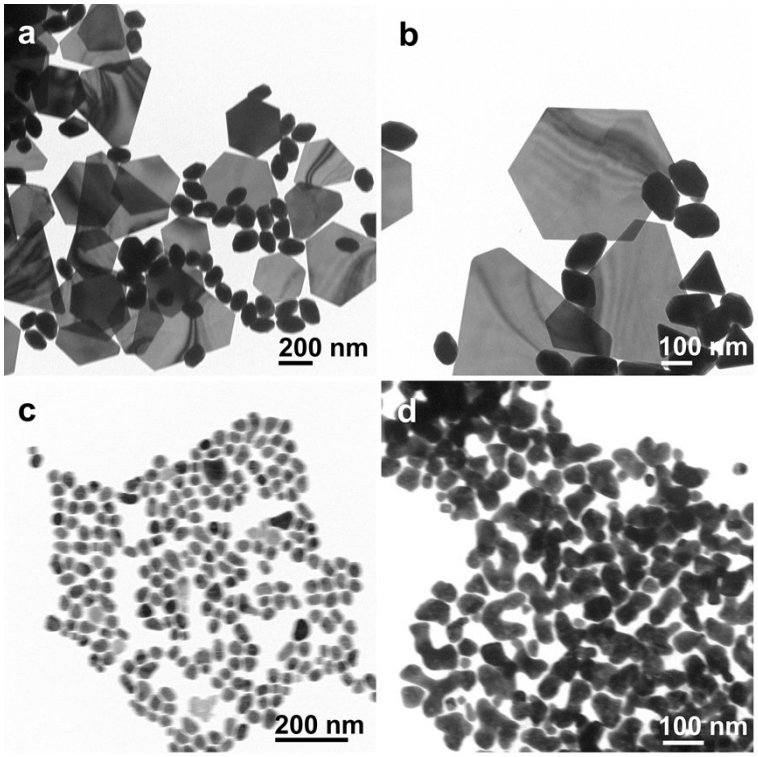

Fig. S5. TEM images of the products with the same reaction conditions as those of the $Pd_{20}Sb_7$ NPs except the use of (a)-(b) NH_4Cl and (c)-(d) NH_4I to take place of NH_4Br.

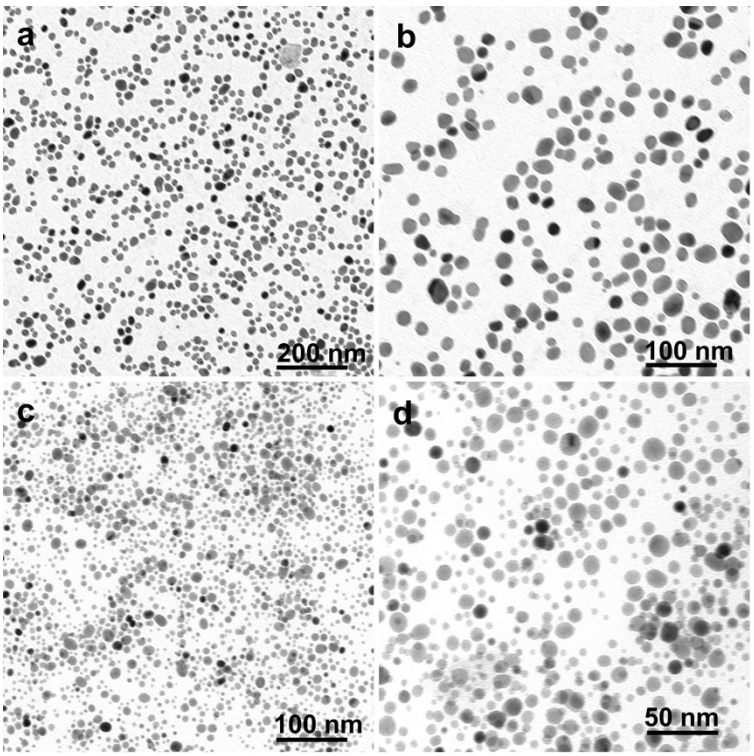

Fig. S6. TEM images of the products with the same reaction conditions as those of the $Pd_{20}Sb_7$ NPs except the use of (a)-(b) DMAC and (c)-(d) EG to take place of DMF.

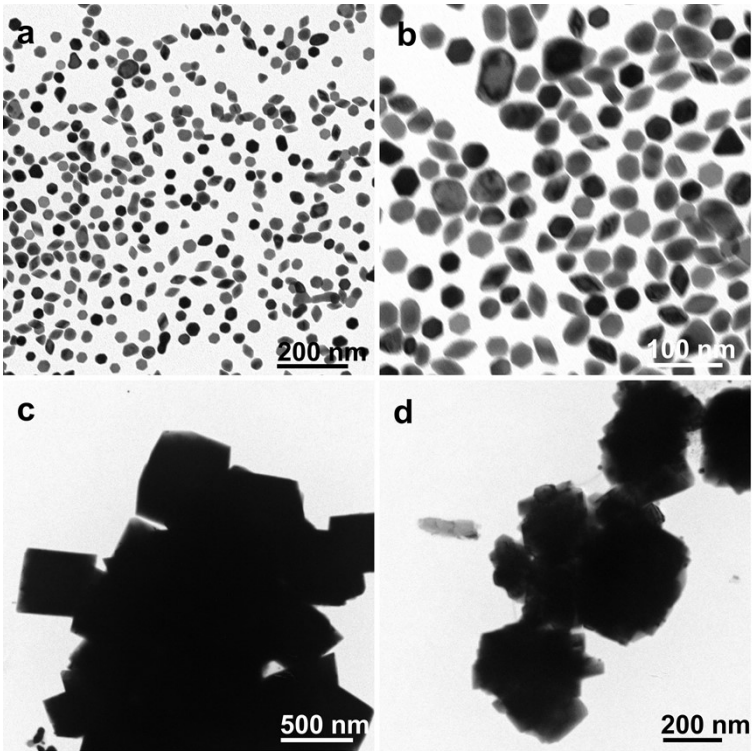

Fig. S7. TEM images of the products with the same reaction conditions as those of the $Pd_{20}Sb_7$ NPs except the use of (a)-(b) $PdCl_2$ to take place of $Pd(acac)_2$ and (c)-(d) $Sb(ac)_3$ to take place of $SbCl_3$.

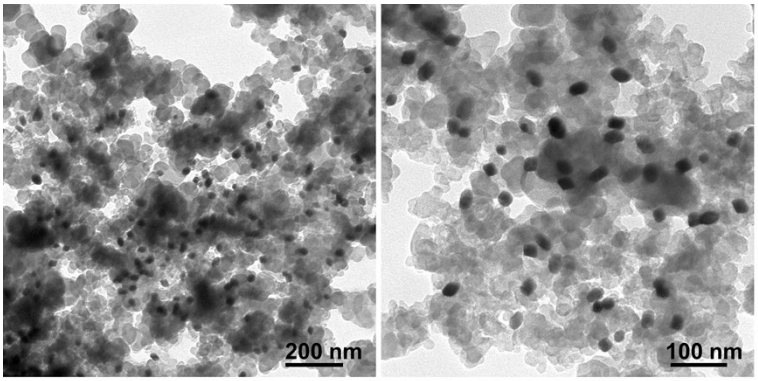

Fig. S8. TEM images of $Pd_{20}Sb_7$ NPs/C.

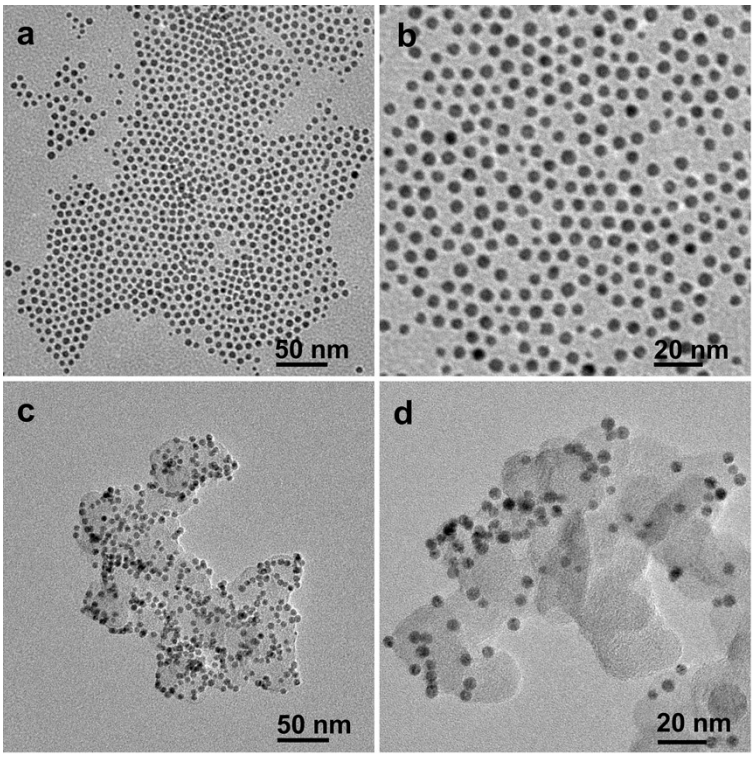

Fig. S9. TEM images of (a)-(b) Pd NPs and (c)-(d) Pd NPs/C.

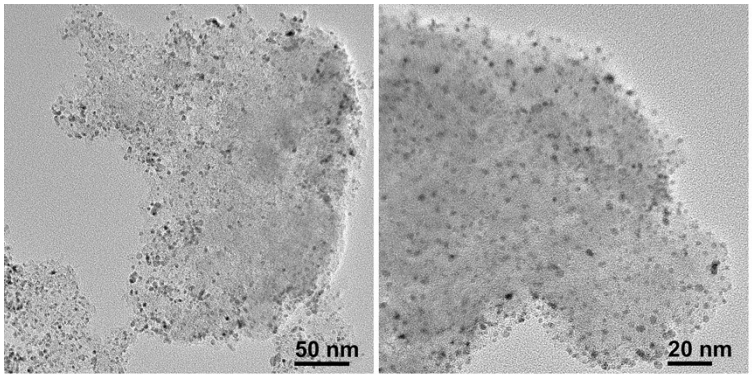

Fig. S10. TEM images of the commercial Pd/C.

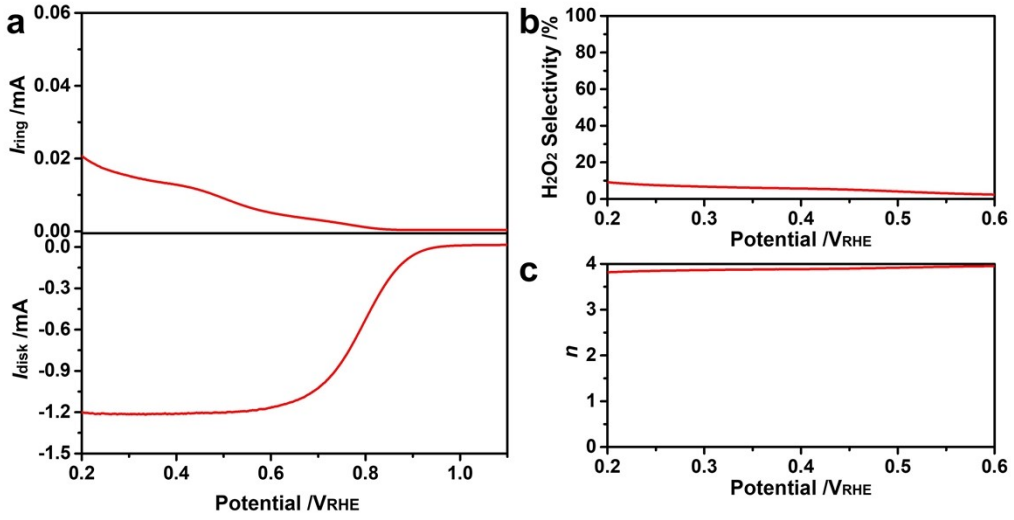

Fig. S11. (a) RRDE voltammograms of $Pd_{20}Sb_7$ NPs/C at 1600 rpm in O_2-saturated 0.1 M KOH with the disk current density and ring current. The scan rate is 10 mV s^{-1}. (b) H_2O_2 selectivity as a function of the applied potential. (c) The calculated values of n as a function of the applied potential.

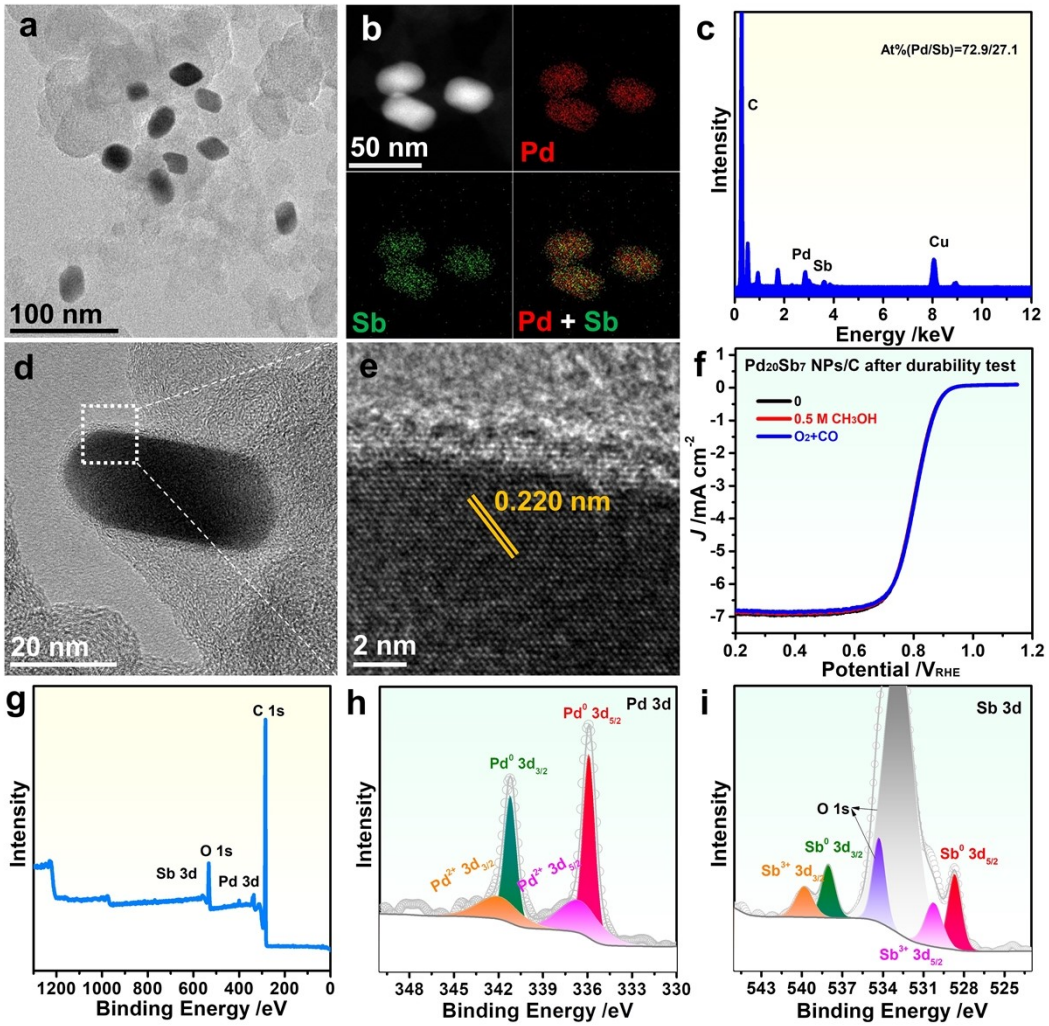

Fig. S12. (a) TEM image, (b) HAADF-STEM image and corresponding element mappings, (c) TEM-EDX spectrum, (d-e) HRTEM images, (f) ORR polarization curves in 0.1 M KOH with 0.5 M CH_3OH or CO, and XPS spectra of (g) survey, (h) Pd 3d, and (i) Sb 3d of $Pd_{20}Sb_7$ NPs/C after durability test.

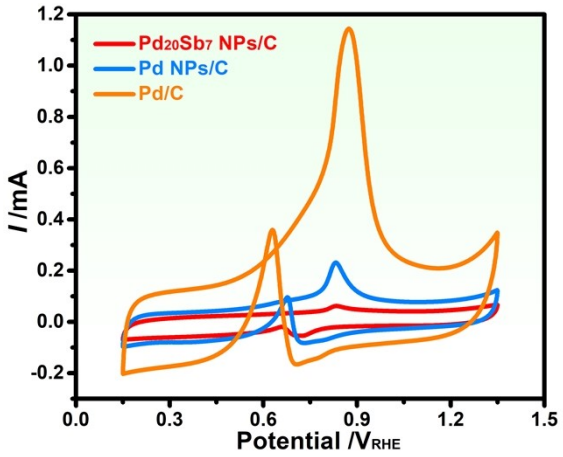

Fig. S13. CVs of $Pd_{20}Sb_7$ NPs/C, Pd NPs/C, and the commercial Pd/C in 0.1 M KOH and 0.5 M CH_3OH solution.

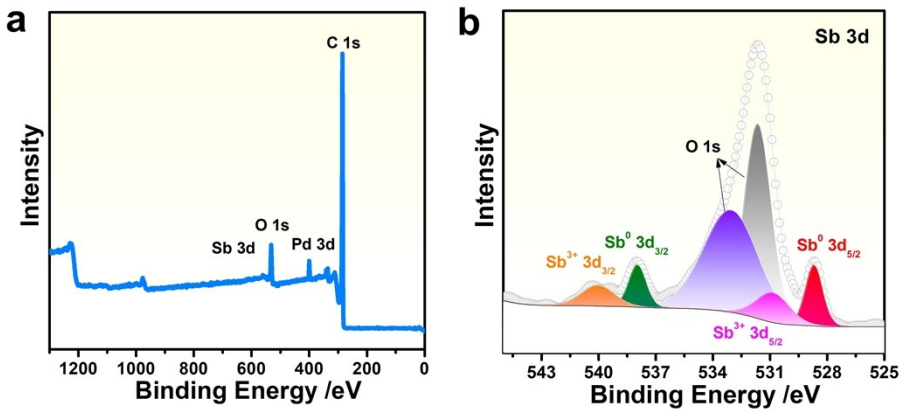

Fig. S14. XPS spectra of (a) survey and (b) Sb 3d of $Pd_{20}Sb_7$ NPs/C.

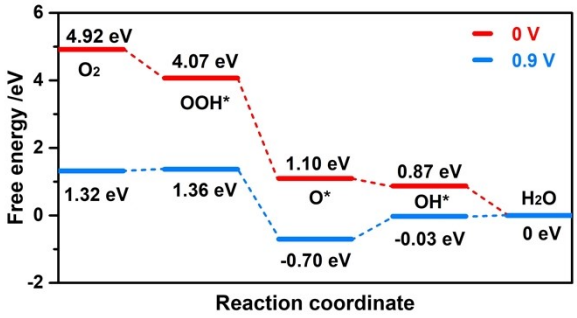

Fig. S15. Calculated free energy profiles at 0 and 0.9 V for ORR on Pd {111} facet, respectively.

Table S1. Curve fit parameters of Pd K-edge EXAFS for Pd powder, $Pd_{20}Sb_7$ NPs/C, and PdO powder.

Sample	Path	CN[a]	R /Å[b]	σ^2 /Å^{2}[c]	ΔE /eV	R-factor
Pd powder	Pd-Pd	12	2.74±0.003	0.005±0.001	-3.42±0.64	0.011
$Pd_{20}Sb_7$ NPs/C	Pd-Sb	3	2.73±0.031	0.009±0.005	2.00±2.38	0.042
PdO powder	Pd-O	4	2.04±0.016	0.003±0.003	3.40±2.17	0.046
	Pd-Pd	4	3.09±0.002	0.002±0.002		

[a]: CN is the coordination number.

[b]: R is the interatomic distance (the bond length between central atoms and surrounding atoms).

[c]: σ^2 is the Debye-Waller factor (a measure of thermal and static in absorber-scatter distances.